IOPscience iopscience.iop.org

Home Search Collections Journals About Contact us My IOPscience

Continuous particle size separation and size sorting using ultrasound in a microchannel

This content has been downloaded from IOPscience. Please scroll down to see the full text.

J. Stat. Mech. (2006) P01012

(http://iopscience.iop.org/1742-5468/2006/01/P01012)

View the table of contents for this issue, or go to the journal homepage for more

Download details:

IP Address: 86.27.188.239
This content was downloaded on 01/08/2015 at 11:25

Please note that terms and conditions apply.

Journal of Statistical Mechanics: Theory and Experiment
An IOP and SISSA journal

Continuous particle size separation and size sorting using ultrasound in a microchannel

Sergey Kapishnikov, Vasiliy Kantsler and Victor Steinberg

Department of Physics of Complex Systems, Weizmann Institute of Science, Rehovot, 76100, Israel
E-mail: sergeyk@wisemail.weizmann.ac.il, Fekantsl@wisemail.weizmann.ac.il and victor.steinberg@weizmann.ac.il

Received 22 November 2005
Accepted 2 January 2006
Published 25 January 2006

Online at stacks.iop.org/JSTAT/2006/P01012
doi:10.1088/1742-5468/2006/01/P01012

Abstract. Continuous separation and size sorting of particles and blood cells suspended in a microchannel flow due to an acoustic force are investigated both numerically and experimentally. Good agreement in the measured particle trajectories in a microchannel flow subjected to the acoustic force with those obtained by the numerical simulations up to the fitting parameter is found. High separation efficiency, particularly in a three-stage microdevice (up to 99.975%), for particles and blood cells leads us to believe that the device can be developed into commercially useful set-up. The novel particle size sorting microdevice provides an opportunity to replace rather expensive existing devices based on specific chemical bonding with an ultrasound cell size sorter that can be considerably improved by adding many stages for multistage size sorting.

Keywords: multiphase flow, microfluidics (experiment), microfluidics (theory)

J. Stat. Mech. (2006) P01012

©2006 IOP Publishing Ltd

Contents

1. Introduction

Increasing needs in biotechnology, environmental science, and medical applications in continuous flow analysis require filtration of basic fluids from particles and cells that can interfere with the on-line analysis. Such continuous flow separators and size sorters are also needed in the fast developing field of microfluidics.

In conventional technological systems such as large scale biotechnological processes, water purification, and particle flow separators, filtration and size sorting are performed either by a centrifuge or by membrane filters that significantly obstruct the continuous flow process. In advanced small scale biotechnological processes particle and cell manipulation is based on much more sophisticated methods that often use specific chemical bonding to extract certain constituents with a high degree of resolution, purity, and effectiveness. Thus, in biotechnology, besides density gradient centrifugation, fluorescent activated cell sorting (FACS), magnetic associated cell separation (MACS), and laser capture microdissection (LCMD) have become the standard methods for cell separation and consistently provide high quality results.

An alternative approach is to exploit physical bulk forces to conduct continuous flow separation and size sorting by using just physical properties of filtered out constituents. Such an approach has the obvious advantages of working in-line as a flow-through separator with rather low flow resistance (in contrast to centrifuge separation and membrane filtration), being suitable for dealing with a wide range of materials, much cheaper, and not specific biochemically in contrast to FACS, MACS, and LCMD mentioned above.

A rather obvious realization of this idea is to use high frequency ultrasonic standing waves to generate a radiation pressure that tends to move particles denser than a fluid toward velocity anti-nodal planes separated by a half a wavelength. This phenomenon is well known though it has not gained widespread technological application since it is highly sensitive to perturbations and involves acoustic forces that are usually rather weak

J. Stat. Mech. (2006) P01012

compared with, e.g., viscous forces in a flow. On the other hand, the well known Kundt figures result from this phenomenon.

The ability of ultrasonic standing waves to manipulate microscopic size particles and cells was demonstrated a long time ago by King [1], further developed theoretically by Yoshioka and Kawashima [2] and Gor'kov [3], and widely investigated experimentally during recent decades [4]. The experimental studies were mostly concentrated on either biological applications or on the development of techniques for harvesting ultrasonically concentrated particles in macroflows. There were numerous attempts to use high frequency ultrasonic standing waves for blood cell sedimentation in containers of the order of millilitres with their subsequent removal. Several techniques were developed for transporting bands of cells or particle clumps along the container axis to achieve efficient cell and particle harvesting. However, these efforts did not lead to practical applications. Only recently has a continuous flow particle filter with 0.25 mm acoustic path length, which corresponds to a single half wavelength, been investigated experimentally [5]. High efficiency separation up to 1000-fold was achieved in a single path filter. The filter was built using conventional engineering techniques suitable for macromachining though the part of the channel where the ultrasound transducer was located, and had dimensions suitable for microengineering.

Our approach is rather different: first, we use the technology of microfluidics to develop a microdevice, and second, we intend to develop a particle size sorter (size spectroscope) rather than separator. Very recently a similar approach to cell separation was also taken in [6].

2. Theoretical background

The forces acting on particles in an acoustic standing plane wavefield are called acoustic radiation forces and can be divided into the primary radiation force acting in an axial direction with respect to the sound propagation, and the secondary particle–particle interaction (Bjerknes) force [7] originating from scattering of the incident wave. The latter is usually negligible compared with the primary force, and it is not taken into account further. When a standing wave is set up in a fluid, the primary acoustic force acting on a particle, whose radius is much smaller than the sound wavelength ($kR \ll 1$, where k is the sound wavenumber), is given in the approximation of zero viscosity by [1]–[3]

$$\bar{F}_{\mathrm{st}} = \frac{2\pi(kR)^3 2\bar{E}_{\mathrm{st}}}{k^2}\Phi(\Lambda,\sigma)\sin 2\vec{k}\vec{r}_0. \tag{1}$$

Here $\bar{E}_{\mathrm{st}}$ is the energy density of the standing waves; $\Lambda = \rho_{\mathrm{p}}/\rho$ is the ratio of the particle ρ_{p} to fluid ρ density; $\sigma = c_{\mathrm{p}}/c$ is the ratio of the sound velocities of a particle, c_{p}, and a fluid, c; R is the particle radius; $\vec{r}_0$ is the vector normal to the force node; and

$$\Phi(\Lambda,\sigma) = \frac{1}{3}\left(\frac{5\Lambda-2}{2\Lambda+1} - \frac{1}{\Lambda\sigma^2}\right). \tag{2}$$

According to the theory, in the field of the standing wave, particles accumulate in nodes of the acoustic force (or in anti-nodes of the velocity field) [1]–[3]. From equations (1), (2) it is seen that the radiation force is proportional to the particle volume and to the acoustic frequency via the wavenumber, k. So, to increase the force acting on a

J. Stat. Mech. (2006) P01012

particle one should use high frequencies up to the megahertz range and higher. Working with high frequency sound is also advantageous for avoiding cavitation. Short wavelength makes this technique suitable and appropriate for implementation in microfluidic channels with characteristic dimensions of the order of a half of a sound wavelength. The short acoustic path length in this case makes the microfluidic channels also more practical from a sound attenuation point of view. For efficient particle separation a laminar flow is used to eliminate transverse mixing by the flow. For a microchannel flow this means a certain limitation on a fluid velocity or rate of fluid discharge. To be on the safe side, it is desirable to keep the Reynolds number, $Re = \rho V d/\eta$, below unity. Here V is the characteristic velocity, η is the dynamic viscosity, and d is the hydraulic diameter of the channel. For our experiments we use a channel of width $a = 160$ μm and depth $b = 150$ μm, $\rho = 1.027$ g cm^{-3}; then for fluid discharge $Q = 100$ nl s^{-1} one gets $Re \simeq 0.7$.

Next, we would like to estimate how fast the interface between a pure fluid and a fluid with particles will be smeared out due to particle diffusion during the passing time of an active part of the channel used for particle separation. The diffusion length traversed by particles during time t can be found from the relation $h = \sqrt{2Dt}$, where D is the particle diffusion coefficient defined as

$$D = \frac{k_{\mathrm{B}}T}{6\pi\eta R}. \tag{3}$$

Here $k_{\mathrm{B}} = 1.38 \times 10^{-16}$ erg K^{-1} is the Boltzmann constant, and T is the temperature. In the case under consideration, the distance between the transducer end and a channel fork is 2 mm. Thus, in our channel the particles cover this distance in $t \approx 0.48$ s at $Q = 100$ nl s^{-1}. So, particles with $R = 5$ μm at $T = 295$ K have the diffusion length $h \simeq 0.2$ μm, i.e. we can neglect the particle diffusion. In the case of a negligible particle diffusion one can readily obtain the solution of a kinetic equation for the probability density function of the particles, ψ [8]. Then the probability distribution function at the velocity anti-node has the form

$$\psi = \psi_0 \exp[t/\tau_{\mathrm{rel}}], \tag{4}$$

where $\tau_{\mathrm{rel}} \equiv 3\eta/4\bar{E}_{\mathrm{st}}\Phi(kR)^2$ is the characteristic relaxation time for the particle distribution dynamics. The energy density in the standing wave can be estimated from the following expression: $\bar{E}_{\mathrm{st}} = 8(\pi f d_{33} U)^2 \rho T_{\mathrm{tr}}$, where $f = kc/2\pi$ is the sound frequency, d_{33} is the longitudinal piezoelectric sensitivity of the transducer, U is the applied voltage on a transducer, and T_{tr} is the transmission coefficient. The energy transmission coefficient depends on impedance matching of materials and interfaces passed by the ultrasound. In the case considered, we used the following sequence of materials: piezotransducer–glass–elastomer–solution, and T_{tr} can be calculated in a step-by-step fashion via the expression $T_{\mathrm{tr}} = 4Z_1Z_2/(Z_1 + Z_2)^2$. As a result, one gets $T_{\mathrm{tr}} = 0.23$, where $Z_{\mathrm{tranc}} = 31.4$ Mrayl, $Z_{\mathrm{glass}} = 13$ Mrayl, $Z_{\mathrm{elas}} = 1.07$ Mrayl, $Z_{\mathrm{solut}} = 1.5$ Mrayl. Using $U = 10$ V and $d_{33} = 290 \times 10^{-12}$ C N^{-1} we obtain finally $\bar{E}_{\mathrm{st}} \simeq 35$ erg cm^{-3} and $\tau_{\mathrm{rel}} \simeq 0.1$ s, which is several times smaller than what is found in the experiment. The main error appears in the estimates of $\bar{E}_{\mathrm{st}}$, since only a small part of it is applied to particles due to partial absorption in surrounding materials, diffraction, interference, and attenuation in the solution. Further we present the results of numerical simulations of particle dynamics in a channel flow subjected to ultrasound standing waves by introducing a fitting parameter that takes into account this discrepancy.

J. Stat. Mech. (2006) P01012

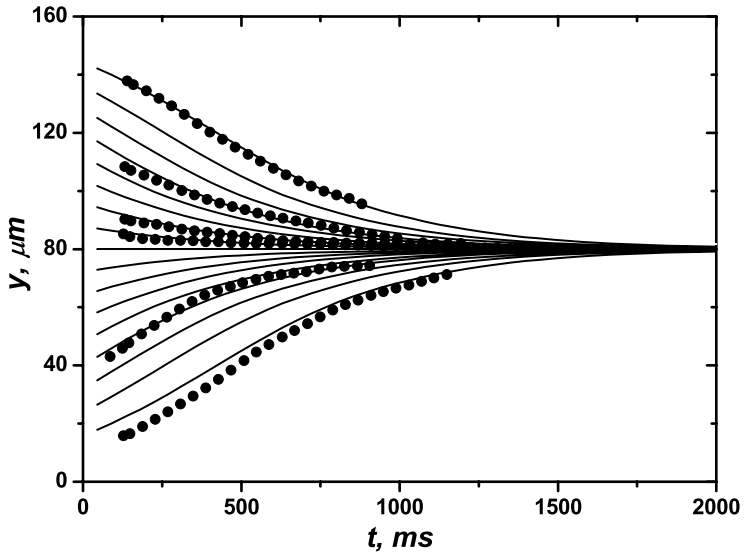

Figure 1. Trajectories of $R = 5$ μm particles in a microchannel as a function of time and initial position. Solid lines represent results of numerical simulations and dots the experimental data.

3. Numerical simulations of particle dynamics in the ultrasound waves

To describe the dynamics of a particle in a channel flow a simple model was suggested. The following equation of particle motion due to the ultrasonic force in a viscous medium:

$$m\ddot{y} = F_{\rm st} \sin(2ky) - C\dot{y} \tag{5}$$

was numerically solved. Here y is the coordinate across the channel, m is the particle mass, $C = 6\pi\eta R$ is the Stokes coefficient, $F_{\rm st}$ is the amplitude of the ultrasonic force that is defined as

$$F_{\rm st} = 4\pi k R^3 \bar{E}_{\rm st} \Phi(\Lambda, \sigma). \tag{6}$$

Using above estimates one gets $F_{\rm st} = 2.5 \times 10^{-6}$ dyn. The temporal dependence of a transverse particle position (perpendicular to the wall of the channel) is shown in figure 1 for various initial particle locations. In order to fit the experimental data, the fitting factor $\beta = 0.2$ was used to correct the estimated value of the energy density and the acoustic force, i.e. we used $\bar{E} = \beta \bar{E}_{\rm st}$ and $F = \beta F_{\rm st}$. So, instead of the estimated value, $F = 5 \times 10^{-7}$ dyn was used for numerical calculations. This gives a relaxation time five times longer and leads to good agreement with the data (see figure 1). We also conducted numerical simulations to determine the clearance coefficient, $K = N_{\rm out}/(N_{\rm in} - N_{\rm out})$, as a function of the flow rate, Q. The former is related to the separation efficiency, $S_{\rm eff} = (N_{\rm out}/N_{\rm in}) \times 100\%$, via the expression $K = S_{\rm eff}(1/(100 - S_{\rm eff}))$, where $N_{\rm in}$ and $N_{\rm out}$ are the initial and final concentrations of particles in the inlet and outlet channels, respectively. In order to carry out these numerical simulations the trajectories of particles in a channel flow also subjected to the acoustic force in the direction transverse to the flow were calculated using equations (5) and (6) and the flow velocity profile in a rectangular

J. Stat. Mech. (2006) P01012

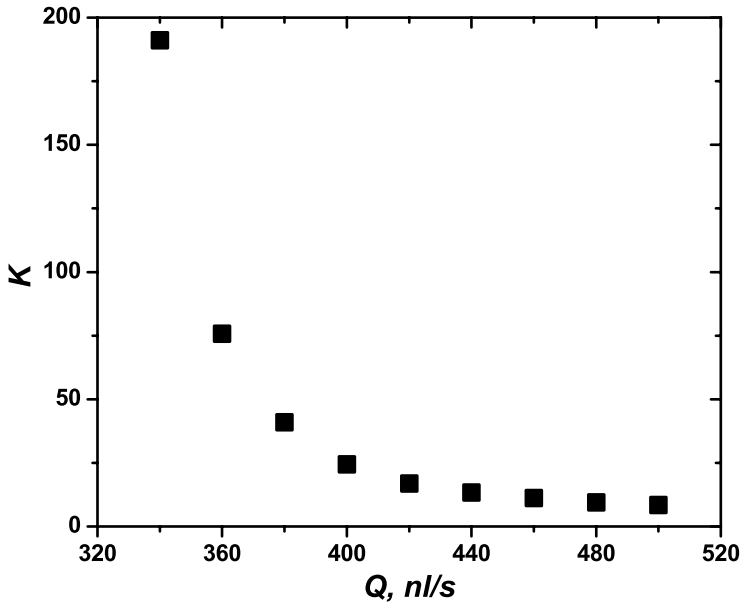

Figure 2. Clearance coefficient as a function of fluid discharge obtained from numerical simulations.

cross-section channel: $-a \le y \le a, -b \le z \le b$, and the flow discharge that is given by the expressions [9]

$$u(y,z) \equiv \dot{x} = \frac{16a^2}{\eta\pi^3}\left(-\frac{\mathrm{d}p}{\mathrm{d}x}\right)\sum_{i=1,3,5,\ldots}^{\infty}(-1)^{(i-1)/2}\left\{1-\frac{\cosh(\mathrm{i}\pi z/2a)}{\cosh(\mathrm{i}\pi b/2a)}\right\}\frac{\cos(\mathrm{i}\pi y/2a)}{i^3}, \tag{7}$$

and

$$Q = \frac{4ba^3}{3\eta}\left(-\frac{\mathrm{d}p}{\mathrm{d}x}\right)\left\{1-\frac{192a}{\pi^5 b}\sum_{i=1,3,5,\ldots}^{\infty}\frac{\tanh(\mathrm{i}\pi b/2a)}{i^5}\right\}. \tag{8}$$

Here we assume that a particle follows a fluid element in the flow direction, x, without any delay, so the particle and fluid velocities in the x-direction are the same, $\dot{x} = u(y,z)$, and gravity is neglected. The numerical calculations of $K(Q)$ were conducted for a rectangular cross-section microchannel with the transducers 1 cm long with one inlet and the flow splitter as the outlet (see figure 4(a)). Using the numerical solution for a large number of particles with different initial locations in the direction transverse to the flow and assuming that all particles that reach the area of the velocity anti-node are extracted from the flow, one can get the dependence of the clearance coefficient on the fluid discharge. The results of the numerical calculations of $K(Q)$ are shown in figure 2.

4. Experimental methods and materials

The experiments on particle separation and size sorting (size spectroscopy) were performed in microchannels. Moulds for the microchannels were produced by a soft lithography technology [10] using UV-sensitive epoxy (SU-8). A microfluidic chip was made of a silicone elastomer Sylgard 184 (the specific gravity is 1.05 g cm^{-3} at 25 °C, the linear

J. Stat. Mech. (2006) P01012

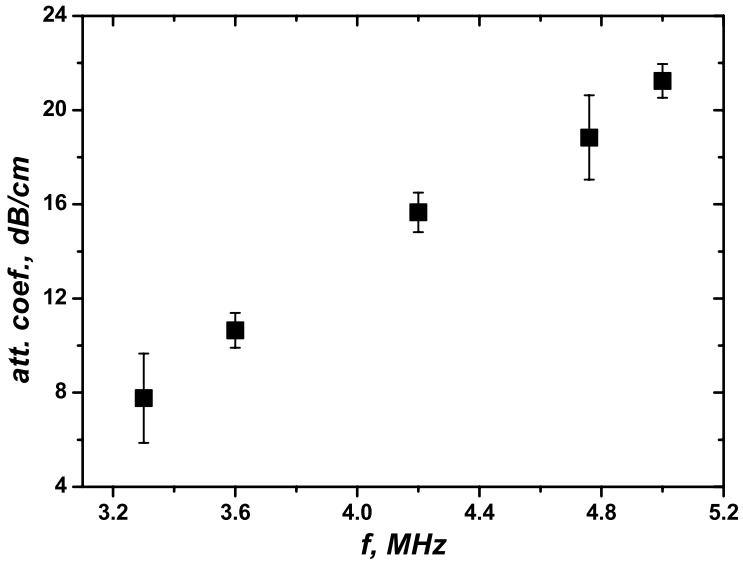

Figure 3. Experimental frequency dependence of the sound attenuation coefficient in the elastomer.

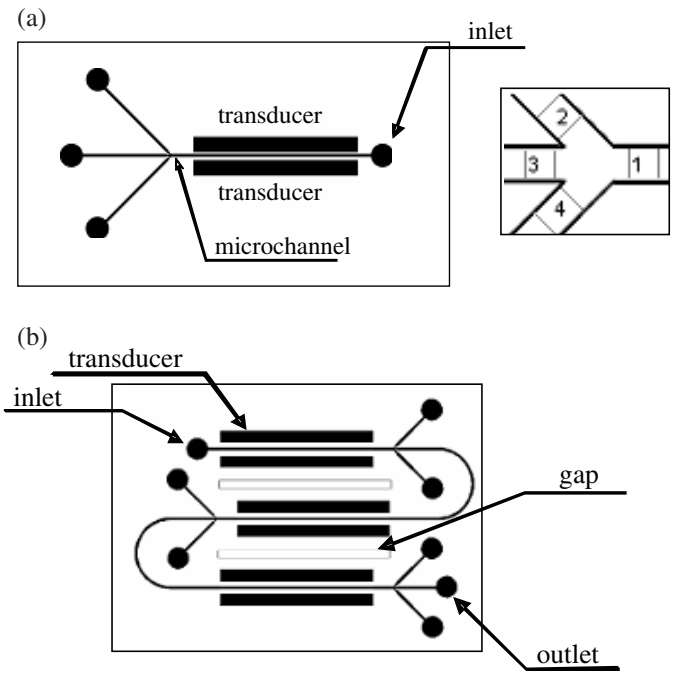

Figure 4. Schematic view of (a) the one-stage microchannel for particle separation using ultrasound and (b) the three-stage microdevice for particle separation.

thermal expansion coefficient is 3×10^4 cm/cm/°C) with a curing time of 4 h at 65 °C. The width of the microchannel for particle and red blood cell separation is 160 μm (about a half of the sound wavelength, λ) and the depth is 150 μm. For the size sorting the design is different and the channel width should be of the order of $\lambda/4$ (about 100 μm; see further

J. Stat. Mech. (2006) P01012

for a detailed explanation), so the channel cross-section in this case is 100×120 μm^2. Transducers (Ferroperm Piezoceramics, type PZ26) were used as emitters of ultrasound waves. Optimal impedance matching between transducers and a solvent can be achieved by adding several layers of quarter-wavelength matching materials with consequently reduced values of acoustic impedance between piezoceramics (31.4 Mrayl) down to water (1.5 Mrayl). By adding $\lambda/4$ layers of lead (24 Mrayl), glass (13 Mrayl), and Mylar (3 Mrayl) one can reach the total transmission coefficient $T_{\rm tr} \simeq 0.41$. We did not try to reach optimal impedance matching in these experiments (i.e. to select the intermediate materials with impedances Z_i chosen according to the expression $Z_i = \sqrt{Z_{i-1}Z_{i+1}}$) and used just a very thin glass slide which results in the total transmission coefficient $T_{\rm tr} \simeq 0.23$. A pair of transducers aligned parallel to a microchannel was used (instead of a transducer and a reflector) in order to create a standing wave and to have control over the position of the node by changing the phase difference between pulses of the same frequency applied at the transducers. The transducers were mounted on both sides of a microchannel in air pockets produced in the elastomer via the soft lithography at a distance 800 μm from the centre of the channel. Sinusoidal signals, applied to the transducers, were obtained from two phase-locked function generators (Hewlett Packard, model 3325B), and amplified by an RF power amplifier (IntraAction, model PA-4). The positions of the nodes were changed by adjusting the phase difference between the signals. The transducers were calibrated by reciprocal methods. We would like to point out that in order to increase the driving force for the particle separation, we used driving amplitudes for the sound transducers that were as large as possible. The limiting factor in this case turns out to be a temperature increase of the solution that can reach tens of degrees. So, in order to control the temperature a precise small thermistor was incorporated into the elastomer. In order to estimate the sound amplitude in the solution we also measured the sound attenuation coefficient as a function of the frequency in MHz range for the elastomer, and RTV (silicone resin) and Perspex (lucite) for comparison. The frequency dependence of the attenuation coefficient is close to linear for the elastomer (see figure 3) and close to that of Perspex although the values are considerably larger than for RTV. In order to get a precise and stable flow rate, a flow rate controller was built. A solution is loaded into a microsyringe moved by a stepping motor, which is driven by the stepping motor controller (Panther L12). The latter was connected to a PC via a COM port and operated using MATLAB software.

Commercially available $R = 5 \pm 1$ μm particles (ORGASOL 2002 EXD NAT 1, ultrafine powder of polyamide 12, with a narrow particle size distribution and nearly round particle shape) were used for a particle separation experiment. Similar particles of $R = 2.5$ and 10 μm were also used in size sorting experiments. Their properties are: density $\rho_{\rm p} = 1.03$ g cm^{-3}; sound velocity: $c_{\rm p} = 2.4 \times 10^5$ cm s^{-1}. In order to dissolve the particles in a water solution the following protocol was used: surfactant (MAFO CAB—BASF)—6.8%; polymeric dispersant (polyacrylate salt, Darvan 7—Vanderbilt)—2.5%; defoamer (Plurafac RA40—BASF)—1.4%; water—89.3%.

Particles were observed using a Leitz Orthoplan polarized microscope. The microchannel was fixed on the translational stage of the microscope. A CCD camera (Panasonic, model BP310 with built-in shutter) and s frame grabber (Ellips RIO) were used in order to capture and digitize images. The pixel size was 2.2×1.1 μm^2 with the 4× objective. In the size sorting experiments the pixel size was 1.2×0.6 μm^2 with the 10× objective and CCD camera Cohu 4710. Solutions at different particle concentrations

J. Stat. Mech. (2006) P01012

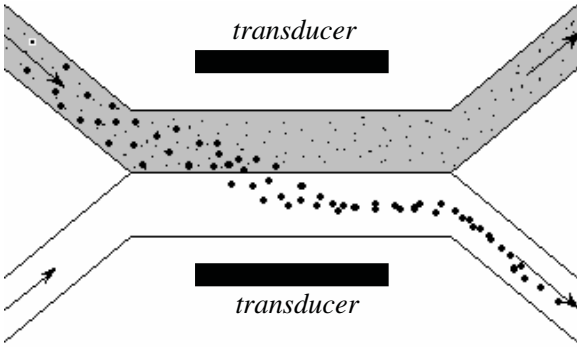

Figure 5. Schematic view of a device for particle size sorting.

were prepared according to the protocol. The solution was loaded into the syringe of the flow rate controller connected to the channel via microtubes. The experiments were conducted at the several flow rates, Q: 54, 81, 90, 108, 135, 162 and 190 nl s^{-1}. Images were processed by two algorithms using MATLAB software. The first algorithm was based on detection of a particle shape and counting of the number of particles at five specific locations in the channels. The clearance coefficient, K, was calculated as the concentration ratio of emerging (central outlet channel) and remaining particles in the filtered solution (two side outlet channels). The number of particles per volume in a certain part of the channel was used to define the concentration of particles in this part of the channel. The second algorithm was based on a calculation of the intensity profile due to particle light scattering across a certain part of the channel. Then the clearance coefficient was calculated as the ratio of the intensity integrals. Each method was chosen depending on certain conditions, such as the particle concentration, quality of images, and the number of emerging particles.

Two designs of the microfluidic separators were used. In the one-stage device (figure 4(a)) separation of suspended particles from a solvent or blood cells from a plasma occurs between two parallel transducers that are located in the inlet channel 1 and produce the field of the ultrasonic standing wave with the force anti-nodes determined by the phase difference between signals generated by the transducers and located near the walls. Then the filtered pure solvent is evacuated via channels 2 and 4 and the concentrated solution with particles via the central channel 1 of the flow splitter. A schematic view of the device is shown in figure 4(a).

The three-stage device works in the same way (see figure 4(b)). The particle separation here occurs on each stage of the separator. On each stage most of the particles (or blood cells) in the solution being affected by the ultrasonic standing waves are directed to the side channels of the flow splitter, while the diluted solution flows via the central channel and passes to the second stage for further dilution and separation. This occurs due to the location of the velocity anti-nodes in this case near the channel walls. In this way we can achieve three-level separation of the solvent from particles (or plasma from the blood cells). The flow rate at the next stage of the channel is three times less then at previous one if all cross-sections of the channels are the same, which also improves the filtering efficiency. In order to avoid interference of sound waves from various pairs of transducers, air-filled gaps between transducers were made (figure 4(b)). For size sorting a different

J. Stat. Mech. (2006) P01012

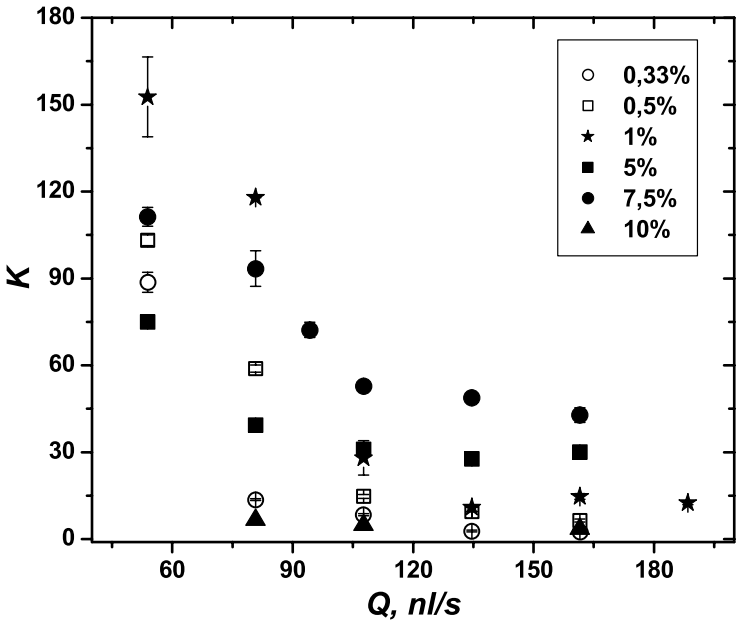

Figure 6. Clearance coefficient as a function of fluid discharge obtained experimentally for six different volume concentrations of particles with $R = 5$ μm.

microchannel was designed (figure 5). It is based on an idea that the particle velocity strongly depends on its size (see equations (5) and (6)); the larger particles move faster through an interface between a pure solvent and solution of different size particles. It is also reflected in the strong dependence (as $\sim R^{-2}$; see equation (4)) of the characteristic time for a particle to relax into a stationary state under the ultrasonic force. To provide a preferred motion of the large size particle through the interface into a pure solvent flow part, the velocity node plane should be located at the wall on the solution side that corresponds to the maximum acoustic force, whereas the velocity anti-node plane should be placed at the opposite channel wall on the pure solvent side (see figure 5). Thus, the channel width should be of the order of $\lambda/4$ in size. In this way one can efficiently separate particles of different sizes. The channel can be built as either a one-stage device (figure 5) or a many-stage one to enhance the size sorting. Of course, the same device can be used for size sorting of various blood cells in the plasma.

5. Experimental results

5.1. Continuous particle separation

First, we carried out measurements of particle trajectories in a microchannel flow for different initial locations of the particles of $R = 5$ μm. The experimental results were found to be in good agreement if the fitting parameter $\beta = 0.2$ was introduced to correct for the acoustic energy density (or the acoustic force) which can be obtained theoretically only at the transducer (see figure 1). Then the experiments on particle separation for six different volume concentrations of particles with $R = 5$ μm, starting from 0.33% and going up to 10% were conducted. The experimentally obtained dependences of the clearance

J. Stat. Mech. (2006) P01012

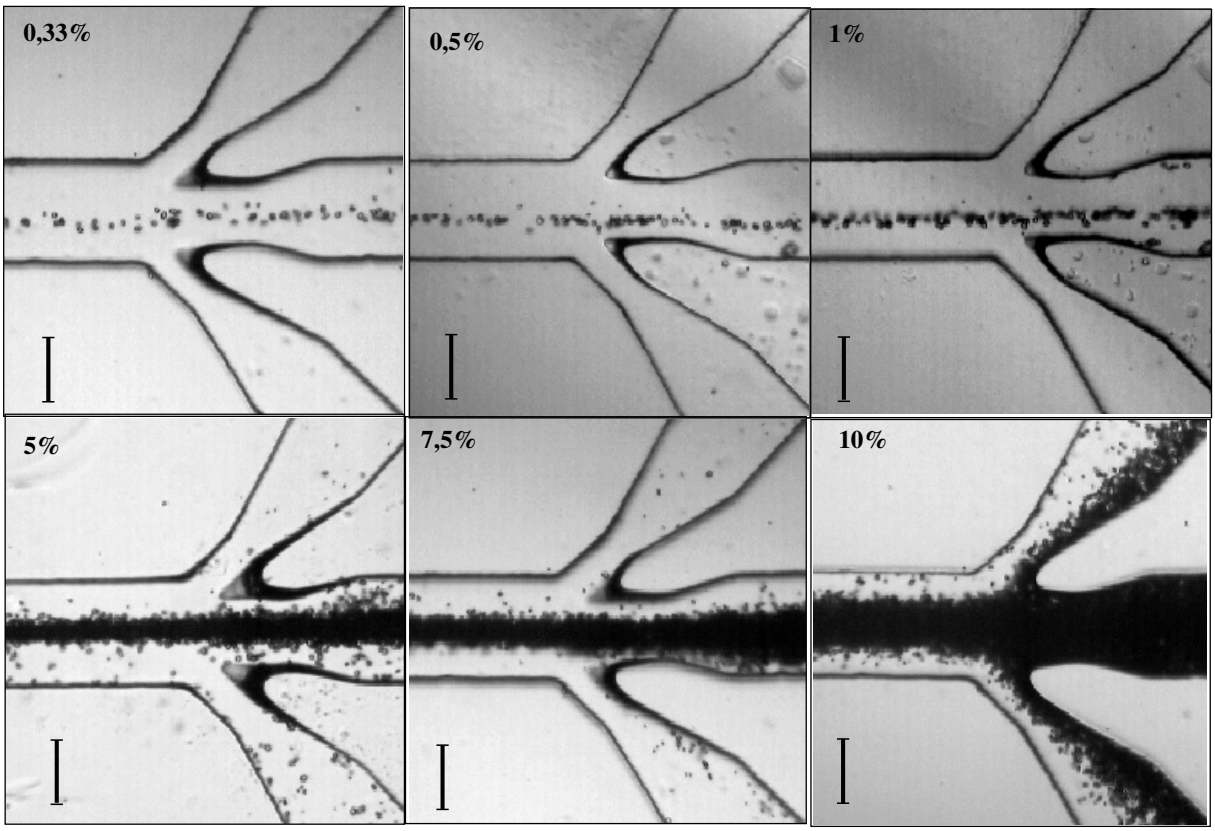

Figure 7. Captured images of particle separations in 0.33%, 0.5%, 1%, 5%, 7.5%, and 10% (by volume) solutions of particles with $R = 5$ μm. The black line is for 100 μm.

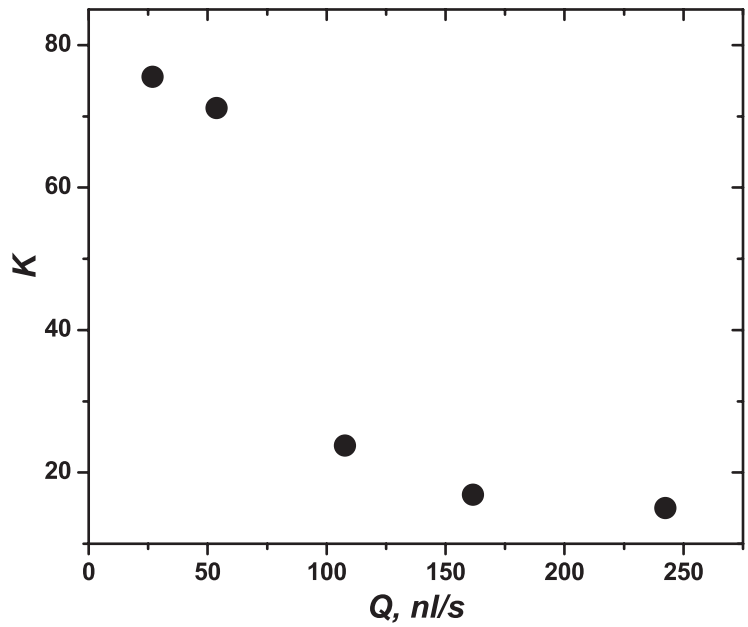

Figure 8. Clearance coefficient as a function of fluid discharge obtained experimentally for a 25% solution of rabbit's blood in PBS.

J. Stat. Mech. (2006) P01012

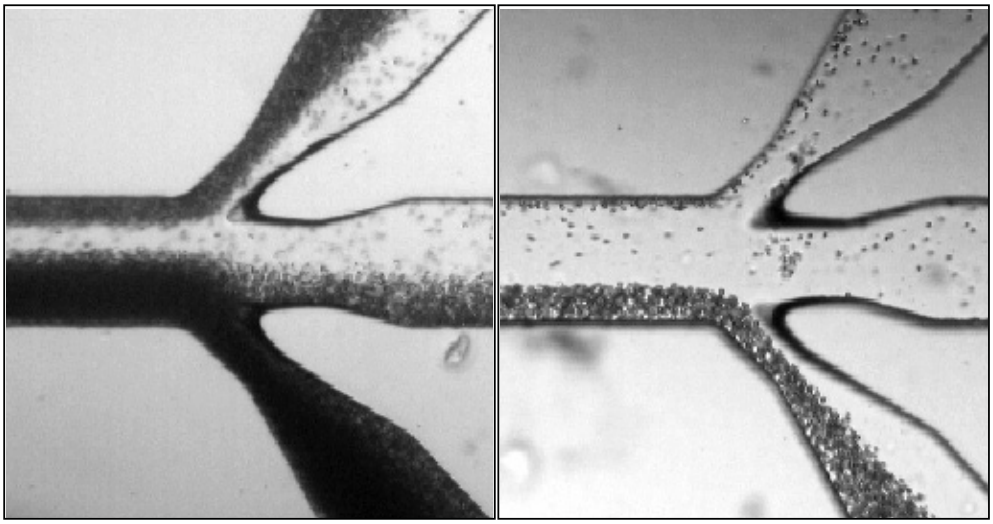

Figure 9. Captured images of blood cell separation from the plasma in the three-stage microdevice: in the first stage (left), and in the second stage (right).

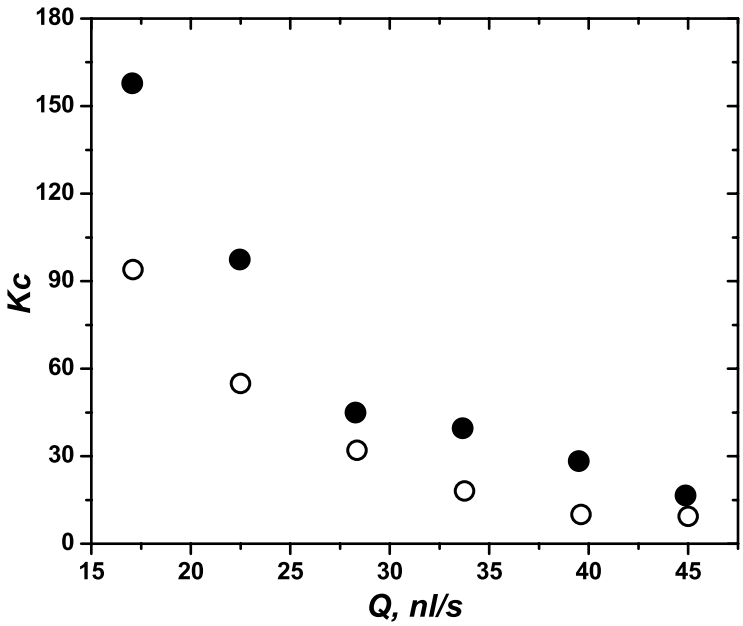

Figure 10. Size sorting coefficient as a function of fluid discharge obtained experimentally for large ($R = 10$ μm) and small ($R = 2.5$ μm) particles for two volume concentrations: open circles, 7.2%; full circles, 1.2%.

coefficient $K(Q)$ on the flow discharge (figure 6) are generally of the same type as those obtained by the numerical simulations (figure 2). However, they differ in absolute value for different concentrations for several reasons. First of all, the absolute values of $K(Q)$ for 0.33% are smaller then those for higher concentrations up to 7.5% due to the casual particles that are located outside the velocity anti-node. Their destructive contribution to K is larger for smaller concentrations than for higher ones. For this reason the values of K

J. Stat. Mech. (2006) P01012

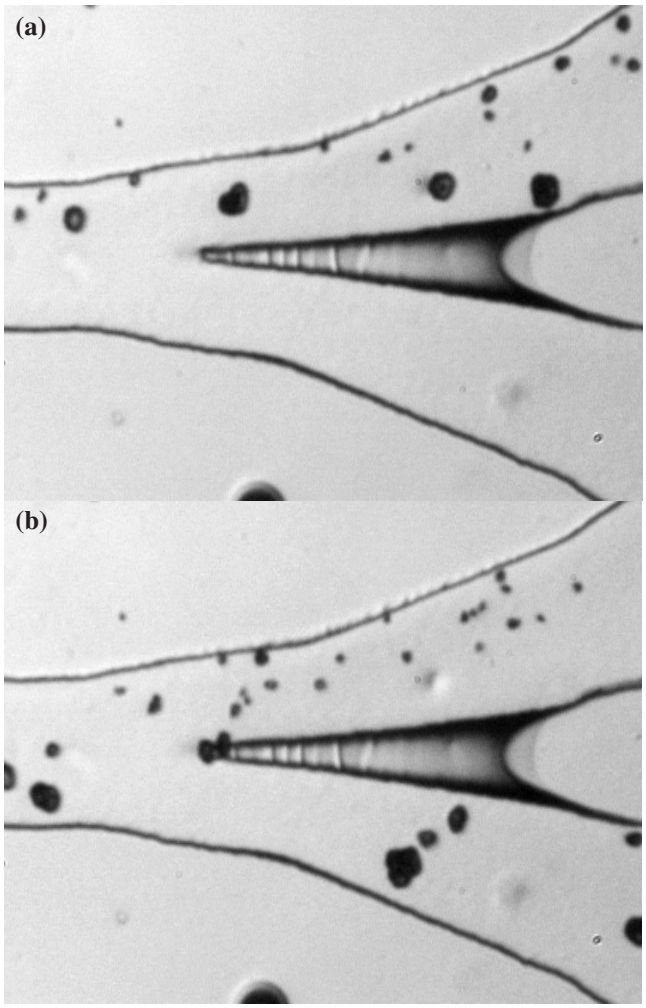

Figure 11. Captured images of size particle sorting for particle concentration 1.2%: (a) without an ultrasonic signal; (b) with an ultrasonic signal.

are the highest for 1% of the particle concentration. The next factor, which affects K, is the scattering of ultrasonic waves on particles. Thus, naturally, for higher concentrations it is higher than for the lower ones. The relative volume of particles in solution, due to their concentration, also affects the separation efficiency. The captured images of particle separation from the solvent for six particle concentrations in a one-stage microchannel are shown in figure 7.

Using the three-stage separation device (figure 4(b)) we were able to achieve the value of $K = 3826$ at the flow rate $Q = 162$ nl s^{-1}.

5.2. Continuous blood cell separation from plasma

The goal of the second group of experiments was to use both our one-stage and our three-stage set-up for separation of blood cells from the plasma. In this case a solution of 25% rabbit's blood in PBS (phosphate buffered saline) was used. The first part of these experiments was done with a blood solution in the one-stage channel. The corresponding

J. Stat. Mech. (2006) P01012

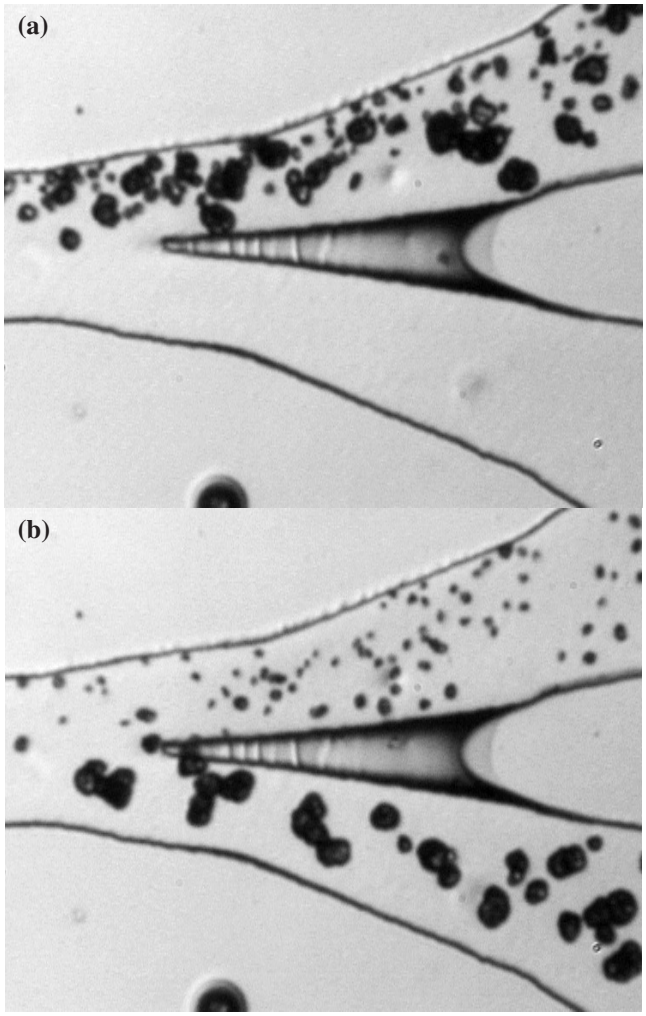

Figure 12. Captured images of size particle sorting for particle concentration 7.2%: (a) without an ultrasonic signal; (b) with an ultrasonic signal.

dependence of $K(Q)$ is shown in figure 8. The second part was done in the three-stage device (figure 4(b)) in order to get higher values of K. Then the maximum value of K reached was about 4000. The corresponding captured images are presented in figure 9.

5.3. Continuous particle size sorting

The ultimate goal of the experiments was to obtain particle size sorting in a microchannel due to the ultrasonic force. We performed an experiment in the microchannel whose schematic design is presented in figure 5. We would like to emphasize here once more that in the case of the size sorting the channel width is about $\lambda/4$ with the velocity anti-node plane located close to the channel wall on the pure solvent side (see figure 5). Such a structure of the acoustic field in the channel and the device design lead to a maximum driving acoustic force on the large particles and provide optimal size sorting. Two values of particle concentration were used. The corresponding size sorting coefficient, $K_c = N_{lout}/(N_{lin} - N_{lout})$, as a function of the flow discharge is shown in figure 10. Here

J. Stat. Mech. (2006) P01012

N_{lout} and N_{lout} are the concentrations of large particles in the outlet and inlet channels, respectively. The captured images of the size sorting are presented for 1.2% in figure 11 and for 7.2% in figure 12 ((a) without an ultrasound signal and (b) with an ultrasound signal).

6. Conclusions

We demonstrated in this paper that the ultrasonic separation of particles and blood cells from a solution in a microchannel is a rather efficient and promising method. Good agreement in the measured particle trajectories in a microchannel flow subjected to acoustic force with those obtained by the numerical simulations up to the fitting parameter is found. High separation efficiency, particularly in a three-stage microdevice, for particles and blood cells leads us to believe that the device can be developed into a commercially useful set-up. Indeed, the maximum clearance coefficient $K \simeq 4000$ corresponds to $S_{\mathrm{eff}} \simeq 99.975\%$ which is comparable with the blood cell separation for commercially available centrifugation. Moreover, the novel particle size sorting design provides an opportunity to replace rather expensive existing devices with an ultrasound cell size sorter that can be considerably improved by adding many stages for multistage size sorting.

References

[1] King L, *On the acoustic radiation pressure on spheres*, 1934 *Proc. R. Soc.* A **147** 212
[2] Yoshioka K and Kawashima Y, *Acoustic radiation pressure on a compressible sphere*, 1955 *Acoustica* **5** 167
[3] Gor'kov L, *On the forces acting on a small particle in an acoustic field in an ideal fluid*, 1962 *Sov. Phys. Dokl.* **6** 773
[4] Coakley W, *Ultrasonic separations in analytical biotechnology*, 1997 *Trends Biotechnol.* **15** 506
[5] Hawkes J and Coakley W, *Forced field particle filter, combining ultrasound standing waves and laminar flow*, 2001 *Sensors Actuators* B **75** 213
[6] Petersson F *et al*, *Continuous separation of lipid particles from erythrocytes by means of laminar flow and acoustic standing wave forces*, 2005 *Lab Chip* **5** 20
[7] Groschl M, *Ultrasonic separation of suspended particles. I. Fundamentals*, 1998 *Acta Acust.* **84** 432
[8] Higashitani K, Fukushima M and Matsuno Y, *Migration of suspended particles in plane stationary ultrasonic field*, 1981 *Chem. Eng. Sci.* **36** 1877
[9] White F, 1991 *Viscous Fluid Flow* 2nd edn (Boston, MA: McGraw-Hill)
[10] Xia Y and Whitesides G, *Soft lithography*, 1998 *Annu. Rev. Mater. Sci.* **28** 153

J. Stat. Mech. (2006) P01012